



Forward-backward asymmetry in the distribution of leptons in $t\bar{t}$ events

The DØ Collaboration
URL <http://www-d0.fnal.gov>
(Dated: July 18, 2013)

We present preliminary measurements of forward-backward asymmetry in the angular distribution of leptons from top and antitop quark decays in $t\bar{t}$ events produced in proton-antiproton collisions at a center-of-mass energy of 1.96 TeV. We consider the final state containing one lepton and at least three jets. The entire sample of data collected by the D0 experiment at the Fermilab Tevatron Collider, corresponding to 9.7 fb^{-1} , is used. The asymmetry measured for reconstructed leptons is $A_{\text{FB}}^l = (3.2 \pm 2.0 \text{ (stat.) } {}_{-1.2}^{+1.4} \text{ (syst.)})\%$. When corrected for detector effects the asymmetry is found to be $A_{\text{FB}}^l = (4.7 \pm 2.3 \text{ (stat.) } {}_{-1.4}^{+1.1} \text{ (syst.)})\%$. We examine the dependence of this asymmetry on the transverse momentum of the lepton. The results are in agreement with predictions from the next-to-leading-order QCD generator MC@NLO.

Preliminary Results for Summer 2013 Conferences

I. MOTIVATION

Previously measured forward-backward asymmetries in $p\bar{p} \rightarrow t\bar{t}(X)$ production [1–3] are in marginal agreement with the predictions of the standard model (SM). This tension has led to many papers exploring its possible causes within and beyond the SM [4].

Within the SM, the asymmetry arises from high order (α_s^3) contributions of quantum chromodynamics (QCD) [5] and from small electroweak corrections [6], yielding predictions of 7 – 9% [7] for the asymmetry defined based on the sign of the rapidity [8] difference of the top quark-antiquark pair, $\Delta y_{t\bar{t}} = y_t - y_{\bar{t}}$. Partial results on the α_s^4 contribution suggest that the correction from the $t\bar{t}$ -jet case [9] might be large, though other publications argue that these may be an artifact [10]. Work on the full calculation of the $t\bar{t}$ cross section to α_s^4 order is ongoing [11], but predictions for the asymmetry are not published yet.

The asymmetry in terms of $\Delta y_{t\bar{t}}$,

$$A_{\text{FB}} = \frac{N(\Delta y_{t\bar{t}} > 0) - N(\Delta y_{t\bar{t}} < 0)}{N(\Delta y_{t\bar{t}} > 0) + N(\Delta y_{t\bar{t}} < 0)}, \quad (1)$$

where N is the number of events satisfying the criteria in the parentheses, was first measured by D0 [12] in the $l+\geq 4$ jet channel. That measurement was superseded by Ref. [1], which found $A_{\text{FB}} = (20_{-7}^{+6})\%$ using a dataset corresponding to an integrated luminosity of 5.4 fb^{-1} . In those measurements, we selected $t\bar{t}(X) \rightarrow W^+bW^-\bar{b}(X)$ events, where one W boson decays hadronically ($q\bar{q}$) and the other decays leptonically ($l\nu_l$). We selected electrons and muons, which may arise directly from the W boson decay or through an intermediate τ lepton. We refer to this $t\bar{t}$ decay chain as the l + jets channel. The CDF collaboration measured A_{FB} in the l +jets [2] and dilepton [3] channels, the combined result being $A_{\text{FB}} = (20 \pm 7)\%$ [13]. CDF also reported a strong rise of A_{FB} with the invariant mass of the $t\bar{t}$ system, $m_{t\bar{t}}$. The asymmetry dependence on $m_{t\bar{t}}$ observed in D0 data [1] was statistically compatible with both the Standard Model prediction and the CDF result.

Previous measurements of the $t\bar{t}$ asymmetry, as defined in Eq. 1, are based on full reconstruction of the $t\bar{t}$ decay chain, and assume on-shell top quarks and that each top quark decays to only three final state fermions. These assumptions limit the comparison of data to theoretical calculations that include higher orders in top quark decay and to those that include off-shell top quarks (e.g., in loops). An alternative to the fully reconstructed, $\Delta y_{t\bar{t}}$ -based asymmetry is the forward-backward asymmetry in lepton production in $t\bar{t}$ events [14],

$$A_{\text{FB}}^l = \frac{N(q_l y_l > 0) - N(q_l y_l < 0)}{N(q_l y_l > 0) + N(q_l y_l < 0)}, \quad (2)$$

where q_l is the electric charge of the lepton and y_l is its rapidity. The above limitations do not apply to this lepton-based asymmetry. From the experimental perspective, it does not require complex event reconstruction or unfolding. The direction of a lepton is determined with far greater precision than that of a top quark; therefore, unfolding is much simpler. Furthermore, with no need for full reconstruction of the $t\bar{t}$ system, the $l+3$ jets sample can be used for this measurement in addition to the previously used $l+\geq 4$ jets sample. This addition almost doubles the number of $t\bar{t}$ events analyzed, at the expense of somewhat lower signal to background ratio. It also reduces the acceptance corrections, which were a leading source of systematic uncertainty.

The lepton-based asymmetry was first measured in the l +jets channel to be $A_{\text{FB}}^l = (15.2 \pm 4.0)\%$ using 5.4 fb^{-1} of data [1]. In the dilepton channel, D0 measured $A_{\text{FB}}^l = (5.8 \pm 5.3)\%$ using 5.4 fb^{-1} of data [15]. The measured A_{FB}^l was significantly larger in the l +jets channel than the SM predictions of 3 – 4% [16]. Motivated by the desire to further investigate this discrepancy, the availability of more data, and by the suggestions that the measurement of the lepton production asymmetry is interesting in its own right [17], we pursue this analysis in greater detail.

Measuring $m_{t\bar{t}}$, the $t\bar{t}$ invariant mass, as done previously, requires full reconstruction of the $t\bar{t}$ system. However, we can also study the dependence of the asymmetry on the $t\bar{t}$ kinematics by noting that the transverse momentum of the lepton, p_T^l , is strongly correlated with $m_{t\bar{t}}$, and can also be used to compare data to the predictions from different models [17]. The observable p_T^l can readily be studied in $l+3$ jet events and is measured with far greater accuracy than $m_{t\bar{t}}$. Thus, this new (doubly) differential measurement is well motivated both experimentally and as a test of new physics models.

We report here an updated measurement of A_{FB}^l , using the full dataset collected by the D0 experiment at Run II of the Fermilab Tevatron Collider, corresponding to 9.7 fb^{-1} after relevant data quality requirements. We extend the measurement to include $l+3$ jet events, improving the background modeling as needed, and measure for the first time the p_T^l -dependence of A_{FB}^l .

II. DEFINING THE LEPTON-BASED ASYMMETRY

In this analysis, we measure the charge (q_l) and rapidity (y_l) of the electron or muon that originates from the W boson from top quark decay. Leptons with $q_l y_l > 0$ are defined as forward and leptons with $q_l y_l < 0$ are defined as backward. We define the lepton-based forward-backward asymmetry in Eq. 2.

The asymmetry can be defined at the reconstruction level, which refers to the measured lepton quantities and is affected by acceptance and resolution. To enable direct comparisons with SM and non-SM calculations, the asymmetry can also be defined at the production level¹, before the modifications made by these effects. All asymmetries are reported after contributions due to background processes are subtracted.

To avoid large acceptance corrections, only events with $|y_l| < 1.5$ are studied here (see Ref. [1]). Thus, the production-level A_{FB}^l is defined including only leptons produced within this “visible phase space” region.

III. ANALYSIS STRATEGY

The inclusion of events that contain only three jets has the advantage of increasing the statistical power of the measurement, as well as making the measurement less susceptible to biases from selection. However, these additional events have a lower signal to background ratio than events with four or more jets. A multivariate algorithm [18] is used to select, or “ b tag”, jets likely to originate from a b quark among the three or four jets with the highest transverse momentum. To maximize the statistical power of the purer subsets, we separate the measurement into several channels, defined by the number of jets (three or at least four) and the number of b -tagged jets (zero, one, or at least two).

The addition of the three-jet events to the analysis also requires improved modeling of the production of W bosons in association with jets (W +jets). The intrinsic asymmetry of the W +jets background depends strongly on the proton’s parton distribution functions (PDFs). We use a top-depleted control sample to calibrate this asymmetry (see Section VIB) and thus reduce the sensitivity of the analysis to the assumed PDFs.

We identify variables that discriminate between $t\bar{t}$ signal and W +jets background separately for $l+3$ jet events and $l+\geq 4$ jet events, and use them to construct a “likelihood” [19] discriminant. Using this discriminant we simultaneously fit the number of $t\bar{t}$ events and the asymmetry A_{FB}^l (see Section VI).

We then correct the $q_l y_l$ distribution for acceptance effects (see Section VII). Since resolutions in lepton direction are excellent, event migrations between $q_l y_l$ categories are negligible and the acceptance corrections suffice for measuring the production-level A_{FB}^l .

In addition to measuring the inclusive A_{FB}^l , we also measure A_{FB}^l in three p_T^l ranges: $20 < p_T^l < 35$ GeV (low), $35 < p_T^l < 60$ GeV (mid) and $p_T^l > 60$ GeV (high). For the p_T^l -dependent measurement we unfold for migrations between different p_T^l ranges before correcting for the effects of acceptance (see Section VII).

IV. EVENT SELECTION

The prototypical $t\bar{t}$ decay in the l +jets channel yields one isolated lepton with a large transverse momentum (p_T), a significant imbalance in transverse momentum (\cancel{E}_T) from the undetected neutrino, and four or more jets: two from the hadronic W boson decay and the other two from fragmentation of the b quarks. Though $t\bar{t}$ events yield four final state quarks in the l +jets decay chain, only partonic final states where the quarks have an angular separation larger than the jet radius² are likely to yield four distinct jets. Even then, one of the jets may be too soft or too forward to pass the selection criteria. Roughly half of the $t\bar{t}$ events have only three jets, and they too are used in this measurement.

We refer to the hadronically decaying top quark as the “hadronic top”, and to the other top quark as the “leptonic top”. Either of these terms can refer to the top quark or the antitop quark. The electric charge of the lepton identifies the electric charge of the leptonic top. The hadronic top is assumed to have the opposite charge.

The event selection criteria used in this analysis are similar to those used to measure the $t\bar{t}$ production cross section in the l +jets channel [20]. The reconstruction and identification of jets, leptons, and \cancel{E}_T is described in Ref. [21]. The e +jets and μ +jets channels have similar event selection requirements. Events are triggered by requiring either a lepton (e or μ) or a lepton and a jet. As in Ref. [20], the criteria for selecting e +jets events are:

¹ Also referred to as the generator level, or the parton level. We maintain the terminology from Ref. [1].

² These are cone jets with a nominal radius of $R = 0.5$ in the η, ϕ plane.

- one isolated electron with $p_T > 20$ GeV and $|\eta| < 1.1$,
- $\cancel{E}_T > 20$ GeV,
- $\Delta\phi(e, \cancel{E}_T) > (2.2 - 0.045 \cdot \cancel{E}_T/\text{GeV})$ radians.

And the criteria for selecting μ +jets events are:

- one isolated muon with $p_T > 20$ GeV and $|\eta| < 1.5$,
- $25 \text{ GeV} < \cancel{E}_T < 250 \text{ GeV}$,
- $\Delta\phi(\mu, \cancel{E}_T) > (2.1 - 0.035 \cdot \cancel{E}_T/\text{GeV})$ radians.

The triangular cuts in the $\cancel{E}_T, \Delta\phi(\mu, \cancel{E}_T)$ plane were optimized to suppress multijet (MJ) production. Events with a second isolated electron or muon in the final state are vetoed.

In addition to the above criteria of Ref. [20] we use the reconstructed uncertainty on the curvature of the track associated with the lepton to require that the sign of the curvature is well measured. This requirement is $\sim 97\%$ efficient for leptons produced in $t\bar{t}$ decay. By studying the distribution of the ratio of the p_T values measured by the calorimetry and by the tracking system, we find that this cut rejects $> 99.9\%$ of the events where the lepton charge was mis-measured. It also reduces the probability of event migration between the three p_T^l bins.

For muons with $p_T^l > 60$ GeV, we also require that the vector sum of the muon momentum and missing transverse energy is greater than 20 GeV. This rejects events consistent with low energy muons from soft jets that were badly reconstructed as having high muon p_T , leading to their misclassification as isolated leptons³. Such events are part of the MJ background, but their modeling as part of that background, using the technique described in Section VIC, is problematic. To limit possible mismodeling, we also suppress these events with additional requirements on the track associated with the muon. Leptons from signal events pass these additional requirements with $\sim 85\%$ efficiency.

Only jets with $p_T > 20$ GeV and $|\eta| < 2.5$ are considered for further analysis, and events are required to contain at least three such jets. The leading jet, that is the jet with the largest p_T , is required to have $p_T > 40$ GeV. As in Ref. [20], in Run IIb we minimize the effect of multiple collisions in the same bunch crossing by requiring that jets are vertex confirmed, i.e., have at least two tracks within the jet cone pointing back to the primary collision vertex. About 70% of the jets that originated from a b quark from top quark decay and about 8% for the other jets in $t\bar{t}$ events are tagged as b jets, as described in Section III.

The main background after this event selection is W +jets production. There is a smaller contribution from MJ production, where jets are misidentified as leptons. Other small backgrounds from single top quark, Z +jets and diboson production are also considered.

We use the MC@NLO event generator [22] combined with HERWIG showering [23] to model the behavior of $t\bar{t}$ events, and ALPGEN [24] combined with PYTHIA [25] to simulate the W +jets background. For the other backgrounds, Z +jets events are simulated with ALPGEN, diboson events are simulated with PYTHIA and events from single top quark production are simulated with COMHEP [26]. The normalizations for the last three background processes are taken from NLO predictions. In the above cases, event generation is followed by the D0 detector simulation and reconstruction. To model energy depositions from noise and additional $p\bar{p}$ collisions within the same bunch crossing, simulated events are overlaid with data from random $p\bar{p}$ crossings according to the distribution of instantaneous luminosity in collider data. The properties of the MJ background are evaluated using control samples from D0 data.

V. THE PREDICTED ASYMMETRIES

As the asymmetry first appears at order α_s^3 , with the largest contribution due to a loop diagram, it is not fully simulated by tree-level event generators. In addition, the modeling of selection and reconstruction effects requires full Monte Carlo (MC) generation. The MC@NLO event generator is well suited for this measurement as it couples a next-to-leading-order calculation of $t\bar{t}$ production with subsequent parton showers to fully simulate $t\bar{t}$ signal events. The simulated asymmetries are listed in Table I separated by jet multiplicity and the number of b tags.

For $t\bar{t}$ signal, the predicted asymmetry decreases as a function of hard gluon emission [1], seen here as a decrease with jet multiplicity. In the case of W +jets background production, W bosons produced via interactions with gluons or sea quarks contribute positively to the asymmetry. On the other hand, W bosons produced via valence-valence collisions contribute negatively to the overall asymmetry. W boson production in association with heavy flavor quarks occurs

³ This issue is irrelevant for electrons, whose kinematics are measured by the calorimetry.

predominantly due to valence-valence collisions, and thus has a lower A_{FB}^l compared to inclusive W -boson production, as shown in Table I for ≥ 1 b tags. Because of the different production mechanisms, the simulated W +jets asymmetries are dependent on PDFs.

TABLE I. Simulated asymmetries for selected $t\bar{t}$ and W +jets events, at reconstruction level. The quoted uncertainties are from the finite sizes of the simulated samples.

Channel	A_{FB}^l (%)	
	$t\bar{t}$ signal	W +jets background
l + jets	1.6 ± 0.1	13.2 ± 0.3
l +3 jets, 0 b tags	2.3 ± 0.4	13.8 ± 0.4
l +3 jets, 1 b tags	2.8 ± 0.3	11.9 ± 0.5
l +3 jets, ≥ 2 b tags	2.7 ± 0.2	7.6 ± 0.9
l + 4 jets, 0 b tags	0.6 ± 0.5	13.1 ± 1.4
l + 4 jets, 1 b tags	1.4 ± 0.3	13.3 ± 1.3
l + 4 jets, ≥ 2 b tags	2.0 ± 0.2	8.2 ± 2.2
l + ≥ 5 jets, 0 b tags	-2.8 ± 1.0	20.1 ± 3.5
l + ≥ 5 jets, 1 b tags	-2.6 ± 0.5	14.5 ± 4.8
l + ≥ 5 jets, ≥ 2 b tags	-2.5 ± 0.5	8.5 ± 7.2

VI. MEASURING THE RECONSTRUCTED A_{FB}

As in the previous measurement [1], we construct a discriminant and perform a maximum likelihood fit over its distribution and the distribution of the sign of $q_l y_l$ to measure the sample composition and the asymmetry. But the asymmetry values measured at this stage, which rely on the simulated asymmetry of the W +jets background, are not used.

Instead, we proceed as follows. We model the composition of the control sample with 3 jets and no b tags using the fit templates, which describe both the signal channels and the control sample, and their fitted normalizations. Using this model, we subtract the non- W +jets processes from the control sample. We calibrate the asymmetry of the simulated W +jets events to the non- W +jets-subtracted control data. Finally, we repeat the maximum likelihood fit using the calibrated W +jets simulation to measure the reconstruction level A_{FB}^l .

A. The discriminant

We choose input variables that

- provide good separation between signal and background;
- are well modeled;
- have little correlation with the lepton rapidity and transverse momentum.

We then combine them to form a “likelihood” discriminant using only their simulated, one-dimensional distributions.

For the l + ≥ 4 jet channels, the discriminant is constructed exactly as in Ref [1]. We first reconstruct the full decay chain using a kinematic fit [27] that varies the observed objects within their experimental resolution to satisfy the constraints imposed by the known W -boson and top-quark masses. We then build the discriminant from the following input variables: a) the χ^2 of the solution chosen by the constrained kinematic fit, b) the transverse momentum of the leading b -tagged jet, or when no jets are b tagged, the p_T of the leading jet, c) $k_T^{\text{min}} = \min(p_T^1, p_T^2) \cdot \Delta R^{12}$, where ΔR^{12} is the distance in the η - ϕ plane between the two closest jets, and p_T^1 and p_T^2 are their transverse momenta, and d) the invariant mass of the jets assigned to the $W \rightarrow q\bar{q}'$ decay in the kinematic fit, calculated using kinematic quantities before the fit. Of these variables, only the χ^2 depends on the lepton, and that dependence is limited as it also depends on the four jets. This discriminant thus has little correlation with p_T^l and $q_l y_l$.

Some of the above variables ((a) and (d)) rely on the full $t\bar{t}$ reconstruction, so for the l +3 jet channels we construct a different discriminant. It is constructed in the same manner, but with the following input variables:

- S — the sphericity, defined as $S = \frac{3}{2}(\lambda_2 + \lambda_3)$, where λ_2 and λ_3 are the two highest out of three eigenvalues of the normalized quadratic momentum tensor M . The tensor M is defined as

$$M_{ij} = \frac{\sum_o p_i^o p_j^o}{\sum_o |p^o|^2}, \quad (3)$$

where p_o is the momentum vector of a reconstructed object o , and i and j are the three Cartesian coordinates. The sum over objects includes the three selected jets and the selected charged lepton. Signal events tend to have higher values of S than background events. Values of S range from zero to one.

- $p_T^{3\text{rd}}$ — the transverse momentum of the third leading jet. This variable tends to have higher values for signal compared to background.
- M_{jj}^{min} — the lowest of the invariant masses of two jets, out of the three possible jet pairings. Jets that arise from gluon splitting are typical of W +jets production and tend to have a low invariant mass. The simulation of this variable in W +jets production will be discussed in Section VIII.
- p_T^{LB} — the transverse momentum of the leading b -tagged jet, or when no jets are b tagged, the p_T of the leading jet.
- $\Delta\phi(\text{jet}_1, \cancel{E}_T)$ — the difference in azimuthal angle between the leading jet and the missing energy. This variable provides additional discrimination between $t\bar{t}$ events, where the escaping neutrino generates most of the missing energy, to the MJ background, where jet energy mis-measurements also contributes significantly to the \cancel{E}_T .

The data distributions in these variables and their modeling are shown in Fig. 1 for selected $l+\geq 4$ jet events and in Fig. 2 for selected $l+3$ jet events. The fractions of $t\bar{t}$ signal, W +jets background and MJ background shown in the figures are taken from the result of the fit described in the next subsection. The fractions for the other backgrounds from Z +jets, single top quark and diboson production are fixed to the predicted number of events.

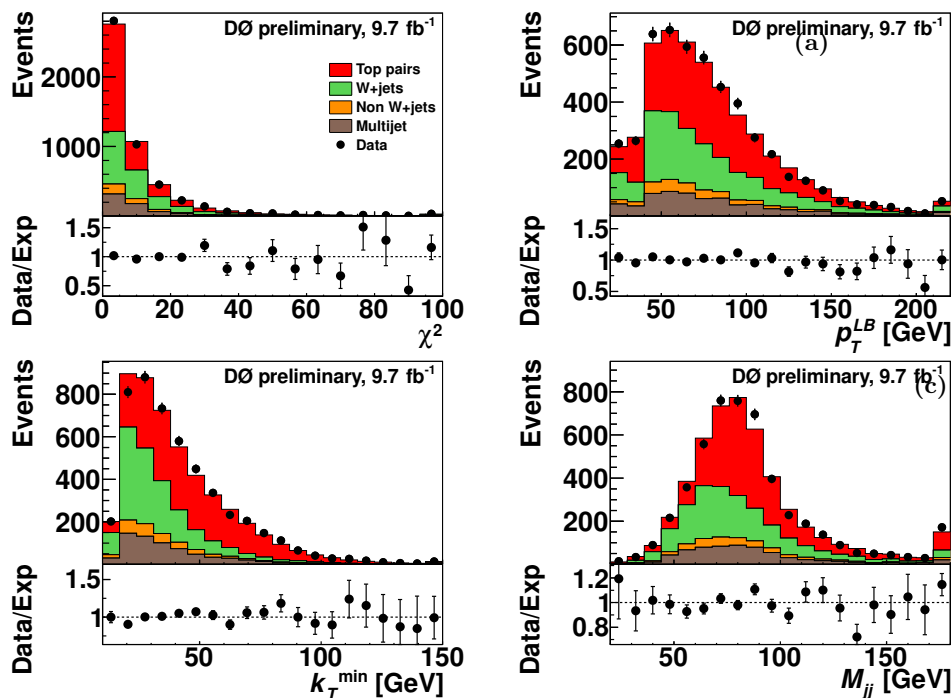


FIG. 1. Input variables to the discriminant in the $l+\geq 4$ jets sample (see Section VIA for details). Overflows are shown in the edge bins. The lower panels show the ratio between the data counts and the model expectations.

B. Calibration of the W +jets background

The measured A_{FB}^l for $t\bar{t}$ events is anti-correlated with the A_{FB}^l assumed for W +jets production in the fit. The W +jets asymmetry differs from channel to channel, mainly due to differences in the flavors of the colliding partons.

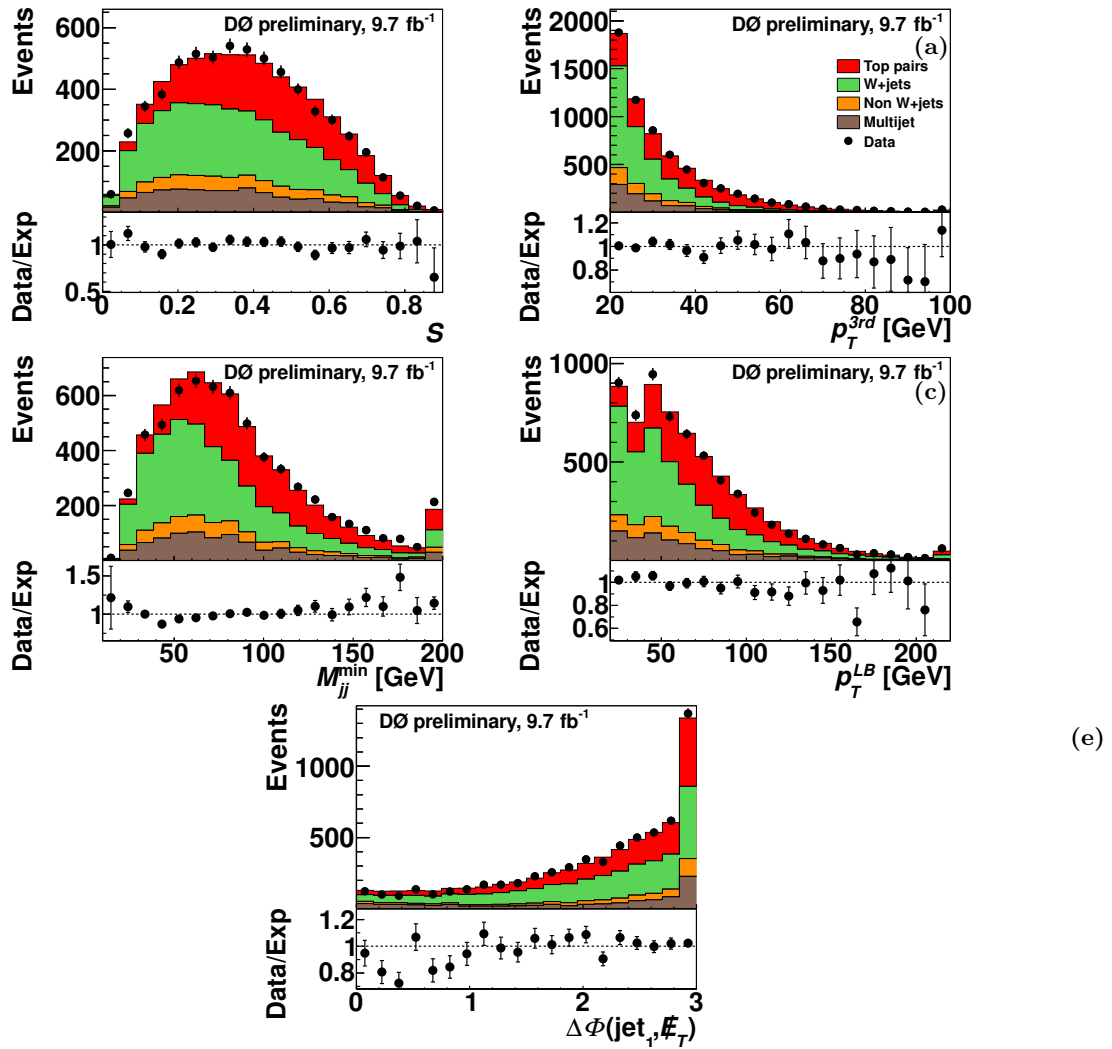


FIG. 2. Input variables to the discriminant in the $l+3$ jets sample (see Section VIA for details). Overflows are shown in the edge bins. The lower panels show the ratio between the data counts and the model expectations.

These flavors are simulated according to the proton's PDFs. To reduce the dependence on the PDFs, we calibrate the simulated A_{FB}^l to three-jet, zero- b -tag data (the control sample), which is used solely for this purpose. The channel-to-channel variations in A_{FB}^l are taken from simulation.

Calibration to data can also reduce other effects. For example, if we do not explicitly account for the backgrounds from Z +jets, single top quark and diboson production, their contributions are attributed to the W +jets background which is calibrated to have an appropriate A_{FB}^l , so that the resulting bias on the measured $t\bar{t}$ A_{FB}^l is only $\approx 0.1\%$.

The distribution of the discriminant in the control sample does not provide reliable information on the sample composition, as the importance of systematic uncertainties on the background shape is magnified by the low signal purity. We extrapolate the results of the fit to the distribution of the discriminant in the signal channels (see Section VIC) to this control sample, and find that it is dominated by W +jets background, with about 70% of events from W +jets production, 20% from MJ production, 9% from other backgrounds and 4% from $t\bar{t}$ production.

We weight the W +jets simulation using the function

$$w = 1 + \alpha q_l y_l,$$

choosing α to match the slope of A_{FB}^l versus $|y_l|$ in the W +jets simulation with the slope in the control sample, after subtracting from the control data the estimated contributions from $t\bar{t}$, MJ and other background production. The uncertainty on α is taken from the statistical uncertainties on the slopes from both data and MC, and is of the same order as the PDF uncertainties.

The production-level measurement is affected by this calibration through the subtraction of W +jets contributions. But the weighting affects the reconstruction-level measurement solely through the changes in the W +jets asymmetry,

ΔA_{FB}^l for W +jets, the difference in the asymmetries from the control sample and the Monte Carlo prediction. These calibration results are listed in Table II. Fig. 3 shows A_{FB}^l versus $|y_l|$ for the W +jets simulation and for data in the control region, along with the uncertainties due to PDFs. It demonstrates that the effects of the calibrations and the PDF uncertainties are of similar sizes.

TABLE II. Results of W +jets calibration

Quantity	Fitted values (%)			
	Inclusive	Low p_T^l	Mid p_T^l	High p_T^l
α	5.2 ± 2.0	9.0 ± 3.1	6.5 ± 2.9	-7.4 ± 4.6
ΔA_{FB}^l	3.1 ± 1.2	5.3 ± 1.8	3.9 ± 1.7	-4.4 ± 2.7

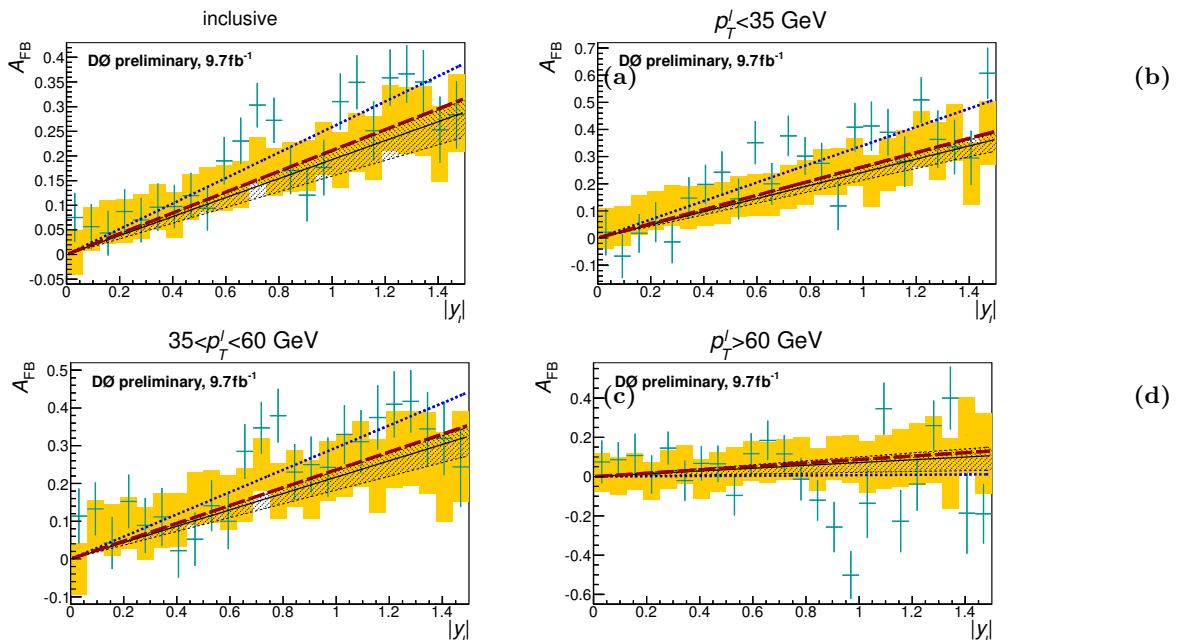


FIG. 3. A_{FB}^l as a function of $|y_l|$ for the W +jets simulation for (a) the inclusive sample, (b) $p_T^l < 35$ GeV, (c) $35 < p_T^l < 60$ GeV, and (d) $p_T^l > 60$ GeV. The blue points and line show the data from the control region, after the subtraction of $t\bar{t}$ and MJ contributions, and their fit. The yellow rectangles show the nominal W +jets simulation, which uses the CTEQ6L1 PDF set [28], and its statistical uncertainty. The dashed, dark red line shows the fit to the nominal simulation. For information only, we also show W +jets simulated with the CTEQ6.1M PDF sets: the black line is the nominal set and the black shaded regions show the sum in quadrature of the PDF uncertainty from the 40 other sets.

C. Maximum likelihood fit

The composition of the data sample and the reconstructed A_{FB}^l are extracted simultaneously using a maximum likelihood fit to the distributions of the discriminant and $\text{sgn}(q_l y_l)$ for events with at least 3 jets and at least one b -tagged jet. The events are separated by the number of jets and the number of b tags into the signal channels, as shown in Fig. 4. The amount of signal in the $l+3$ jets and 0- b -tags channel is insignificant with respect to systematic uncertainties on the background modeling, hence it is excluded from the fit for sample composition.

The following four samples are used to construct the templates for the fit:

- simulated $t\bar{t}$ signal events with $q_l y_l > 0$;
- simulated $t\bar{t}$ signal events with $q_l y_l < 0$;
- simulated W +jets events,

- a control data sample that has been enriched in MJ production by inverting the lepton isolation requirements [20].

The distribution of the discriminant is the same for both signal templates, thus their relative contribution is controlled by the $\text{sgn}(qly_i)$ distribution and corresponds to the fitted reconstruction-level asymmetry, after background subtraction.

The normalization of the MJ background is evaluated using control data and is based on the probability of a jet to satisfy the lepton quality requirements [20]. The probability for jets to pass lepton quality requirements, particularly in the μ +jets channel, is highly dependent on p_T^l . We therefore split the MJ background template into six components, one for each lepton flavor and p_T^l range, defined in Section III. The presence of signal in the control data (“signal contamination”) is accounted for both in the likelihood and when calculating the relative weights of the templates in the data model (e.g., in Figs. 2 and 1). To reduce statistical fluctuations in the p_T^l -dependent measurement, and in other fits of subsamples (see Section IX), the MJ distributions are re-binned in the discriminant.

The results of the inclusive fit, as well as those of fits in the three p_T^l ranges defined in Section III, are listed in Table III. The fitted $N_{t\bar{t}}$ imply a p_T^l distribution consistent with the SM. The distributions of the discriminant are shown in Fig. 4; the distributions of qly_i are shown in Fig. 5.

TABLE III. Predicted A_{FB}^l values and fit results at reconstruction level.

Quantity	Inclusive	Low p_T^l	Mid p_T^l	High p_T^l
Pred. A_{FB}^l (%)	1.6 ± 0.2	1.2 ± 0.4	1.2 ± 0.3	2.3 ± 0.3
A_{FB}^l (%)	$3.2 \pm 2.0^{+1.4}_{-1.2}$	$-0.8 \pm 4.0^{+1.9}_{-2.0}$	$3.2 \pm 3.1^{+1.9}_{-1.3}$	$7.5 \pm 3.5^{+2.1}_{-1.8}$
$N_{W+\text{jets}}$	4475 ± 75	1643 ± 39	1840 ± 46	1008 ± 41
N_{MJ}	959 ± 24	321 ± 13	306 ± 14	332 ± 14
N_{Other}	817	280	332	205
$N_{t\bar{t}}$	4882 ± 71	1362 ± 37	2018 ± 44	1477 ± 39

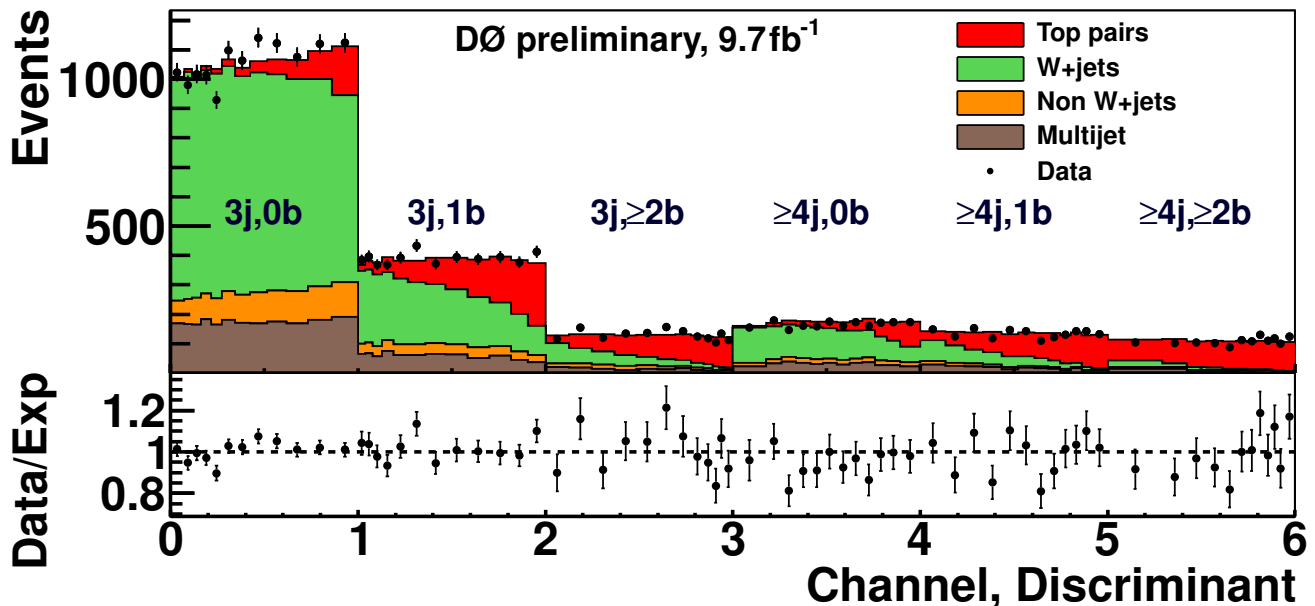


FIG. 4. The discriminant for all channels, side by side. The first three sections of each plot ($0 < D < 3$) correspond to the $l+3$ jet channels, while the last three ($3 < D < 6$) correspond to the $l+\geq 4$ jet channels. Within each category the first section, $0 < D < 1$ and $3 < D < 4$, contains events with 0 b tags, the second one, $1 < D < 2$ and $4 < D < 5$, contains events with 1 b tag, while the third one, $2 < D < 3$ and $5 < D < 6$, contains events with 2 or more b tags. The region $D < 1$ is not used in the fit for sample composition and A_{FB}^l . The ratio between the data counts and the model expectation is shown in the lower panel.

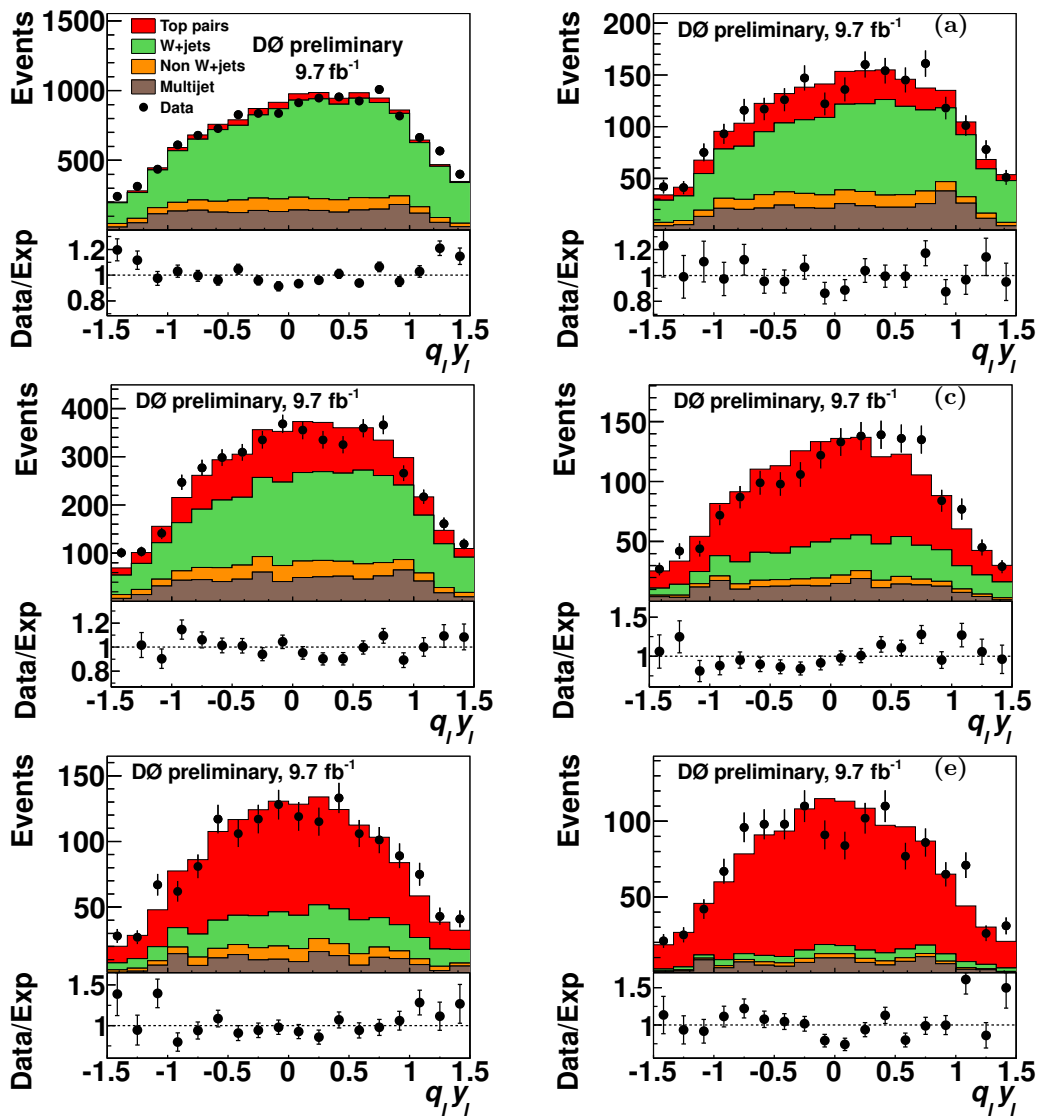


FIG. 5. The $q_l y_l$ distribution for: (a) $l+3$ jets and 0 b tags, (b) $l+\geq 4$ jets and 0 b tags, (c) $l+3$ jets and 1 b tag, (d) $l+\geq 4$ jets and 1 b tag, (e) $l+3$ jets and ≥ 2 b tags, and (f) $l+\geq 4$ jets and ≥ 2 b tags. The ratio between the data counts and the model expectation is shown below.

VII. UNFOLDING THE ASYMMETRIES

We unfold the inclusive A_{FB}^l using a procedure that is almost identical to that used in the previous A_{FB}^l measurement [1]. Due to the excellent angular resolution for leptons, migrations are negligible and unfolding reduces to correcting for acceptance effects. We correct for acceptance by dividing the content of each bin by the selection efficiency for that bin. The efficiencies are taken from MC@NLO, thus these corrections assume the SM as modeled in MC@NLO. As in Ref. [1], to avoid large weights from high $|y_l|$, where the efficiencies are low, we require $|y_l| < 1.5$. To fully describe the selection effects, we divide the range $y_l \in [-1.5, 1.5]$ to 48 uniform bins. In the case of the differential measurement, we unfold for the effects of p_T^l migration via a simple 3-by-3 matrix inversion. The corrections for acceptance and migrations modify A_{FB}^l by at most 0.5%

Unlike the method in Ref. [1], here we have multiple channels with differing statistical strength. We thus correct each channel separately, using channel-specific acceptance corrections.

We evaluate the statistical uncertainty on the unfolded A_{FB}^l from each channel using an ensemble of pseudo-datasets (PDs) that match the size of the data sample and its fitted composition and with the signal simulated according to MC@NLO. The PDs are simulated using Poisson fluctuations both on the selected sample and on the MJ control sample. For the $l+3$ jet channels we find uncertainties of 24.0%, 6.8%, and 4.7%, for 0, 1, and ≥ 2 b tags, respectively.

For the $l+\geq 4$ jet channels we find 13.9%, 4.7%, and 3.6% (in the same order). The $l+3$ jets and 0 b tags channel is used to calibrate the modeling of the W +jets background, and so can not be used to extract the signal A_{FB}^l . We also do not use the $l+\geq 4$ jets and 0 b tags channel for the unfolded result, due to the large uncertainty on A_{FB}^l there. We combine the four b -tagged channels with a weighted average.

The lepton-based asymmetries unfolded to the production level are summarized in Table IV and shown in Fig. 6. The results are compared to MC@NLO-based predictions.

TABLE IV. Predicted and observed production-level lepton-based asymmetries.

Quantity	Inclusive	A_{FB}^l (%)		
		Low p_T^l	Mid p_T^l	High p_T^l
Data	$4.7 \pm 2.3^{+1.1}_{-1.4}$	$-0.2 \pm 4.0^{+1.7}_{-2.3}$	$4.6 \pm 3.5^{+1.8}_{-1.3}$	$9.8 \pm 3.7^{+1.9}_{-2.2}$
MC@NLO	2.3	1.5	2.2	3.1

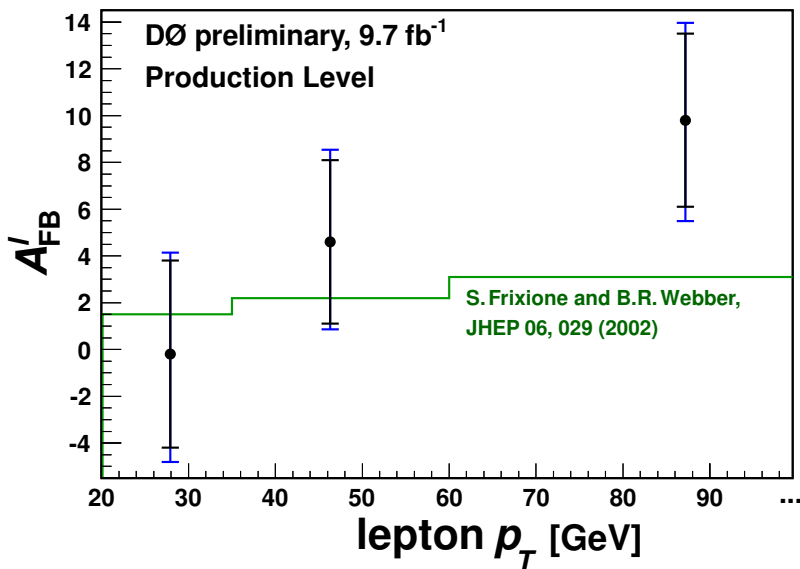


FIG. 6. Predicted [22] and observed production-level lepton-based asymmetries as a function of lepton transverse momentum. The inner error bars represent the statistical error; the outer error bars represent the total error.

VIII. SYSTEMATIC UNCERTAINTIES

We consider multiple sources of systematic uncertainty. For most sources, we vary the modeling according to the evaluated uncertainty, repeat the entire analysis and then propagate the effect to the final result. This accounts for all systematics correlations and anticorrelations between the channels. Some sources are quantified using more specialized procedures. Systematic uncertainties from different sources are added in quadrature to yield the total systematic uncertainties. Table V lists the systematic uncertainties on the reconstruction-level, unfolded, and predicted A_{FB}^l . The main sources are:

Jet reconstruction (reco): This includes the uncertainties on jet reconstruction and identification efficiencies, as well as on the efficiency of the vertex confirmation described in Section IV, all of which are measured using dijet data. We also include the uncertainties on the modeling of multiple $p\bar{p}$ collisions within the same bunch crossing that can yield additional jets.

Jet energy measurement: The jet energy scale (JES) and its uncertainties are measured using dijet and photon+jet samples. The simulated jet energy resolution (JER) is calibrated using Z +jet data, and the uncertainty on this calibration is propagated to this measurement.

Signal modeling: To understand the dependence on the signal simulation, we repeat the analysis using signal events simulated with ALPGEN combined with PYTHIA for all steps but the acceptance correction, where using ALPGEN

rather than MC@NLO would be overly conservative. Being a tree-level generator, ALPGEN lacks the loop diagrams that enhance backward events with no initial state radiation (ISR). Acceptance is lower for events with no ISR [1], so ALPGEN can not predict the forward-backward structure of the acceptance.

Modeling of gluon radiation and color reconnection can affect the dependence of the asymmetry on the transverse momentum of the $t\bar{t}$ system, as the extra radiation can differ between forward and backward events. This difference is controlled by the simulated color coherence of the partonic showers [1], which is somewhat stricter via angular ordering in simulation than expected in QCD [29]. This dependence can affect the measured asymmetry through the sensitivity of the acceptance to $p_T^{t\bar{t}}$. To quantify this uncertainty, we consider the possibility that the dependence of A_{FB}^l on $p_T^{t\bar{t}}$ is 25% smaller than simulated, and find that it is negligible compared to the effect of using a different MC generator. The effect of the uncertainty on the mass of the top quark is also negligible [1].

b tagging: The b -tagging efficiency and mis-tagging probability, which are determined from dijet data with at least one muon identified within a jet, affect the division of events between 0, 1, and ≥ 2 b tags subsamples. Due to this division of channels, the analysis is now more sensitive to the uncertainties from this determination than the previous measurement [1].

Background (Bg) subtraction: The subtracted amounts of W +jets and MJ background are changed within their fitted uncertainties. Uncertainties on the normalization and shape of the MJ background arise from the uncertainties on the lepton selection rates, which are used to evaluate the MJ background. The rate of inclusive $Wc\bar{c}$ and $Wb\bar{b}$ production predicted by ALPGEN must be scaled up by a factor of 1.47 to match the lepton+jets data [20]. The uncertainty on this scale factor is estimated to be 20%.

Background (Bg) modeling: The W +jets background calibration is varied within the uncertainties on the α values as listed in Table II. An excess of data events is seen at the two edge bins on either side of Fig. 5, especially for the control sample. The possibly underestimated fake-high- p_T muon background described in Section IV peaks in that region. We consider the possibility that this excess is due to enhanced MJ production at $|y_l| > 1.13$ by reweighting the MJ $q_l y_l$ distribution to better match the control sample. We similarly consider the possibility that this excess is due to enhanced W +jets production.

We account for the marginal agreement between data and ALPGEN simulation of the dijet invariant mass and the related observables by re-weighting the M_{jj}^{min} distribution in W +jets to match data in the $l+3$ jets and 0- b -tags control region. [30] This improves the modeling of M_{jj}^{min} in all channels, supporting the attributing of the likely (but small) mismodeling of this distribution to the modeling of W +jets production. PDFs are varied within their uncertainties.

TABLE V. Systematic uncertainties on A_{FB}^l . Only uncertainties above 0.1% are listed.

Source	Absolute uncertainty (%)		
	Reconstruction level Prediction	Measurement	Prod. level Measurement
Jet reco	-0.1	-	-0.4
JES/JER	+0.1	+0.2/-0.3	+0.3/-0.5
Signal modeling	-	-	-0.1
b tagging	± 0.1	± 0.3	+0.3/-0.5
Bg subtraction	n/a	+0.2/-0.3	+0.1/-0.5
Bg modeling	n/a	+1.4/-1.0	+1.0/-1.0
Total	± 0.1	+1.4/-1.2	+1.1/-1.4

IX. DISCUSSION

The inclusive lepton-based asymmetry at the production level, which we measure using a dataset corresponding to an integrated luminosity of 9.7 fb^{-1} , is $\left(4.7 \pm 2.3 \text{ (stat.)}_{-1.4}^{+1.1} \text{ (syst.)}\right) \%$. The previously published value, which was measured using 5.4 fb^{-1} of data [1], is $(15.2 \pm 4.0) \%$. Unlike the previous measurement, the current result is in agreement with the MC@NLO prediction of 2.3%. The statistical uncertainty is reduced by a factor of $\approx \sqrt{3}$ with

respect to the published measurement. The statistical strength increased due to the addition of new data and the inclusion of events with three jets.

The inclusion of $l+3$ jet events, the addition of newer data, the use of better object identification algorithms and improvements to the analysis technique all decrease the measured asymmetry. In both analyses, such details were finalized before analyzing Tevatron data. Together, these changes reduce the measured A_{FB}^l by 10.5%, but no single change accounts for a difference of more than 2.5%.

The p-value for the previously published value, assuming the asymmetry predicted by MC@NLO, is 1.3×10^{-3} , while the p-value of the new result is 0.37. These numbers do not account for the systematic uncertainty on the theoretical predictions, nor do they account for the “look elsewhere effect” due to choices of observable (e.g., $\Delta y_{t\bar{t}}$), subsample (e.g., $m_{t\bar{t}} > 450$ GeV as in Refs. [1, 2]), and measure (e.g., $\langle qly_l \rangle$).

Most of the asymmetry in the previous analysis is contained in the $l+\geq 4$ jets channel for events with exactly one b tag. In the current analysis, the asymmetry in this channel is still high, at $(16.5 \pm 4.7(\text{stat.})_{-1.9}^{+1.6}(\text{syst.}))\%$. It is only marginally consistent with the asymmetry in the other channels combined, which is $(1.5 \pm 2.8(\text{total}))\%$. The relative weight of this channel dropped from $\sim 50\%$ in the previous analysis to 24% in the current analysis. The qly_l distributions in each channel were shown in Fig. 5; the A_{FB}^l values of the various channels are compared in Fig. 7, Table VI and Table VII. The consistency between different channels in Fig. 7 corresponds to a χ^2 score of 8.2 for three degrees of freedom, which has a p-value of 4%.

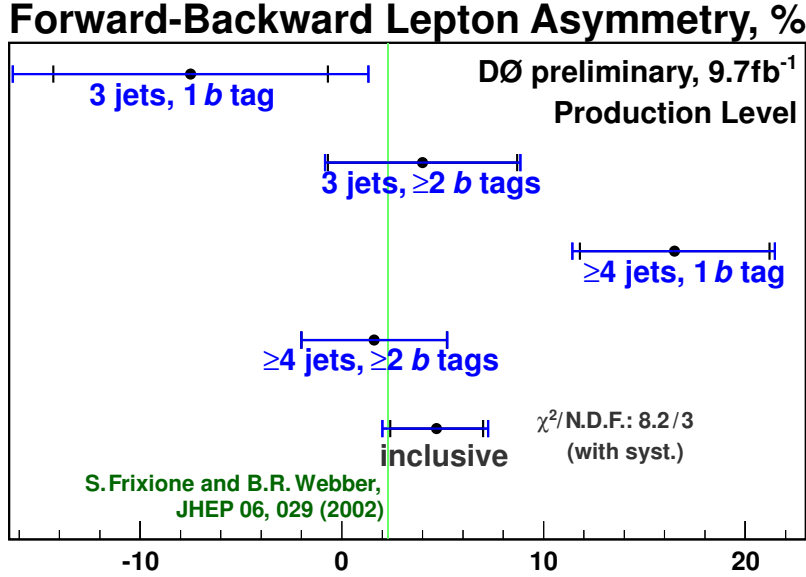


FIG. 7. Measured production-level A_{FB}^l by analysis channel, and the inclusive measurement. The green vertical box shows the MC@NLO prediction [22] with the MC statistical uncertainty. The χ^2 is of a fit of the per-channel results with their total errors to a single value. Statistical uncertainties are indicated by the inner vertical lines, and the total uncertainties by the vertical end lines.

TABLE VI. Measured and predicted A_{FB}^l by channel, at reconstruction level. The errors quoted for the predictions include systematic uncertainties that effect the selection.

Channel	$A_{\text{FB}}^l(\%)$	
	Data	MC@NLO
$l+3$ jets, 1 b tag	$-6.5 \pm 5.9(\text{stat.})_{-4.0}^{+4.6}(\text{syst.})$	2.8 ± 0.3
$l+3$ jets, ≥ 2 b tags	$4.4 \pm 4.2(\text{stat.})_{-0.9}^{+1.0}(\text{syst.})$	2.7 ± 0.3
$l+\geq 4$ jets, 1 b tag	$15.2 \pm 4.1(\text{stat.})_{-1.0}^{+1.0}(\text{syst.})$	0.4 ± 0.3
$l+\geq 4$ jets, ≥ 2 b tags	$-0.3 \pm 3.1(\text{stat.})_{-0.4}^{+0.2}(\text{syst.})$	1.1 ± 0.3
Total	$3.2 \pm 2.0(\text{stat.})_{-1.2}^{+1.4}(\text{syst.})$	1.6 ± 0.2

We also studied the variation of the asymmetry when breaking up the data into independent subsets according to lepton charge, lepton flavor, and the polarities of the detector solenoid and toroid magnets, which are regularly

TABLE VII. Measured A_{FB}^l by channel and predicted A_{FB}^l , at production level.

Channel	$A_{\text{FB}}^l(\%)$	
	Data	MC@NLO
$l+3$ jets, 1 b tag	-7.5 ± 6.8 (stat.) ± 5.6 (syst.)	
$l+3$ jets, ≥ 2 b tags	4.0 ± 4.7 (stat.) $^{+1.2}_{-1.1}$ (syst.)	2.3
$l+\geq 4$ jets, 1 b tag	16.5 ± 4.7 (stat.) $^{+1.6}_{-1.9}$ (syst.)	
$l+\geq 4$ jets, ≥ 2 b tags	1.6 ± 3.6 (stat.) $^{+0.4}_{-0.2}$ (syst.)	
Total	4.7 ± 2.3 (stat.) $^{+1.1}_{-1.4}$ (syst.)	

reversed. Reversing the magnet polarities reduces the possible experimental biases, particularly due to charge tracking asymmetries. All agree within about two standard deviations.

Since the Standard Model-derived corrections are small, the analysis may hold for many beyond the SM scenarios. We tested our analysis method using axigluon samples produced using MADGRAPH combined with PYTHIA at various mass points between 200 GeV and 2 TeV with completely left-handed, completely right-handed and mixed couplings [31]. The axigluon coupling constants were chosen to yield production-level A_{FB} values of $\approx 10\%$ and a wide range of A_{FB}^l values: from -6 to 16% . In these axigluon scenarios, the bias due to SM corrections is typically less than 2% .

X. CONCLUSIONS

Using the full Tevatron data sample, corresponding to 9.7 fb^{-1} of D0 data, we measure the lepton-based forward-backward asymmetry in $t\bar{t}$ events and compare it to a prediction based on MC@NLO. The lepton-based asymmetry does not require a full reconstruction of the $t\bar{t}$ event. Taking advantage of this fact we extend the measurement to the $l+3$ jet subsample. The measured asymmetry at production level is $(4.7 \pm 2.3 \text{ (stat.)}^{+1.1}_{-1.4} \text{ (syst.)})\%$, in agreement with the MC@NLO prediction of 2.3% . Most of the strong asymmetry observed in the 5.4 fb^{-1} analysis [1] was due to events with at least four jets and exactly one b tag. In the current analysis, with about twice the statistics, the asymmetry in this channel is still high (16.5 ± 5.0)%, but marginally consistent with the combined asymmetry seen in the other channels (1.5 ± 2.8)%. We also present the first measurement of the differential asymmetry as a function of p_T^l , whose results are in agreement with MC@NLO predictions.

ACKNOWLEDGMENTS

We thank G. Perez, M. Mangano and P. Skands for enlightening discussions. We thank the staffs at Fermilab and collaborating institutions, and acknowledge support from the DOE and NSF (USA); CEA and CNRS/IN2P3 (France); MON, NRC KI and RFBR (Russia); CNPq, FAPERJ, FAPESP and FUNDUNESP (Brazil); DAE and DST (India); Colciencias (Colombia); CONACyT (Mexico); NRF (Korea); FOM (The Netherlands); STFC and the Royal Society (United Kingdom); MSMT and GACR (Czech Republic); BMBF and DFG (Germany); SFI (Ireland); The Swedish Research Council (Sweden); and CAS and CNSF (China).

-
- [1] V. M. Abazov *et al.* (D0 Collaboration), Phys. Rev. D **84**, 112003 (2011).
 - [2] T. Aaltonen *et al.* (CDF Collaboration), Phys. Rev. D **83**, 112003 (2011);
T. Aaltonen *et al.* (CDF Collaboration), Phys. Rev. D **87**, 092002 (2013).
 - [3] <http://www-cdf.fnal.gov/physics/new/top/2011/DilAfb/cdfpubnote.pdf>
 - [4] A recent review is J. A. Aguilar-Saavedra, Nuovo Cim. C **035N3**, 167 (2012) [arXiv:1202.2382 [hep-ph]].
 - [5] J. H. Kuhn and G. Rodrigo, Phys. Rev. Lett. **81**, 49 (1998).
 - [6] W. Bernreuther and Z. G. Si, Nucl. Phys. B **837**, 90 (2010);
W. Hollik and D. Pagani, Phys. Rev. D **84**, 093003 (2011).
 - [7] See also: N. Kidonakis, Phys. Rev. D **84**, 011504 (2011);
V. Ahrens *et al.*, Phys. Rev. D **84**, 074004 (2011).
 - [8] The rapidity y is defined as $y(\theta, \beta) = \frac{1}{2} \ln [(1 + \beta \cos \theta) / (1 - \beta \cos \theta)]$, where θ is the polar angle and β is ratio of a particles momentum to its energy.
 - [9] S. Dittmaier, P. Uwer and S. Weinzierl, Phys. Rev. Lett. **98**, 262002 (2007).
 - [10] K. Melnikov and M. Schulze, Nucl. Phys. B **840**, 129 (2010).
 - [11] M. Czakon, A. Mitov, J. High Energy Phys. **1301**, 080 (2013);
M. Czakon, A. Mitov, J. High Energy Phys. **1212**, 054 (2012).
 - [12] V. Abazov *et al.* (D0 Collaboration), Phys. Rev. Lett. **100** 142002 (2008).
 - [13] http://www-cdf.fnal.gov/physics/new/top/2011/AfbComb/Afb_combo_5invfb.pdf
 - [14] M. T. Bowen, S. D. Ellis and D. Rainwater, Phys. Rev. D **73**, 014008 (2006).
 - [15] V. Abazov *et al.* (D0 Collaboration), Phys. Rev. D **87**, 011103(R) (2013).
 - [16] W. Bernreuther and Z. -G. Si, Phys. Rev. D **86**, 034026 (2012).
 - [17] A. Falkowski, M. L. Mangano, A. Martin, G. Perez and J. Winter, arXiv:1212.4003 [hep-ph].
 - [18] V. Abazov *et al.* (D0 Collaboration), Nucl. Instrum. Methods Phys. Res. A **620**, 490 (2010). In this analysis, jets with $MVA > 0.035$ are tagged.
 - [19] V. M. Abazov *et al.* (D0 Collaboration), Phys. Rev. D **83**, 032009 (2011).
 - [20] V. M. Abazov *et al.* (D0 Collaboration), Phys. Rev. D **84**, 012008 (2011).
 - [21] V. Abazov *et al.* (D0 Collaboration), Phys. Rev. D **76**, 092007 (2007).
 - [22] S. Frixione and B. R. Webber, J. High Energy Phys. **06**, 029 (2002);
S. Frixione *et al.*, J. High Energy Phys. **08**, 007 (2003).
 - [23] G. Corcella *et al.*, J. High Energy Phys. **01**, 010 (2001).
 - [24] M. L. Mangano *et al.*, J. High Energy Phys. **07**, 001 (2003).
 - [25] T. Sjöstrand *et al.*, Comput. Phys. Commun. **135**, 238 (2001).
 - [26] E. Boos *et al.* (CompHEP Collaboration), Nucl. Instrum. Meth. A **534**, 250 (2004).
 - [27] S. Snyder, Doctoral Thesis, State University of New York at Stony Brook (1995).
 - [28] J. Pumplin *et al.*, J. High Energy Phys. **07**, 012 (2002);
D. Stump *et al.*, J. High Energy Phys. **0310**, 046 (2003).
 - [29] J. Winter, P. Z. Skands and B. R. Webber, J. High Energy Phys. **1207**, 151 (2012).
 - [30] e.g., the jet ΔR reweighting of T. Aaltonen *et al.* (CDF Collaboration), Phys. Rev. D **82**, 112005 (2010).
 - [31] J. Alwall, M. Herquet, F. Maltoni, O. Mattelaer and T. Stelzer, JHEP **1106**, 128 (2011).